Testing and Optimization of Magnetoelectric Devices

Effects of DC Biasing on WPT and Biomagnetic Sensing Performance

Ann Bonde, BMEn & Comp Sci., University of Minnesota
Dr. Troy Olsson, ESE

Motivation

Sensitive Biomagnetic Sensor

- For magnetocardiogram (MCG), magnetomyography (MMG), and magnetoencephalogram (MEG)
- Biomagnetic signals range in amplitude and frequency as shown in Figure 1, requiring very high sensitivity
- Superconducting QUantum Interference Devices (SQUIDs) limited by cryogenic cooling

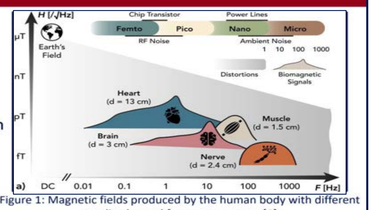

Figure 1: Magnetic fields produced by the human body with different amplitudes and frequency ranges. [1]

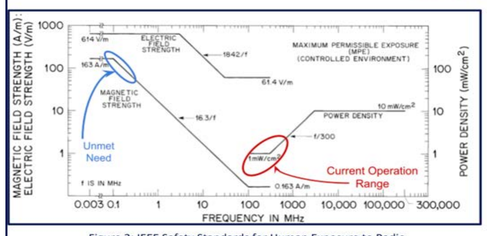

Figure 2: IEEE Safety Standards for Human Exposure to Radio Frequency Electromagnetic Fields [2].

High Efficiency Wireless Power Transfer

- Need small footprints, high efficacy, operate at safe frequencies, and allow longer ranges
- Current coupled coil systems have low Q-factors and high resonance, forcing operation with low power, in the region shown in red in Figure 2.

Introduction

Magnetostrictive (MS) and Piezoelectric (PE) Materials

MS materials experience strain due to the rotation of molecular magnetic dipoles. Magnetic domains within the material orient to align with changes in the field, producing deformations in the whole material.

PE materials produce a charge differential when experiencing material stress. The atomic crystal structure elongates or compresses from the resulting strain. The charge distribution becomes asymmetrical in the unit cell, causing a polarization to appear in the direction of the force. Aluminum Nitride is one such PE material, with the crystal mechanism shown in Figure 3. This occurs throughout the bulk of the material, causing a net voltage change to occur across the sample.

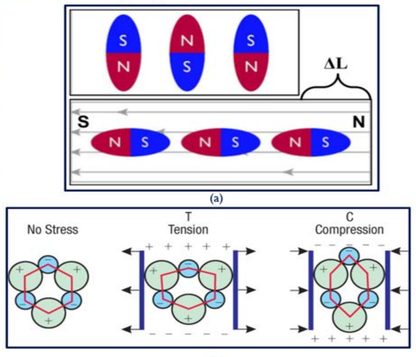

Figure 3: Basic mechanisms of (a) MS and (b) PE materials [3].

Magnetoelectric (ME) Device

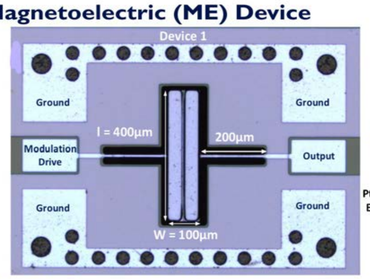

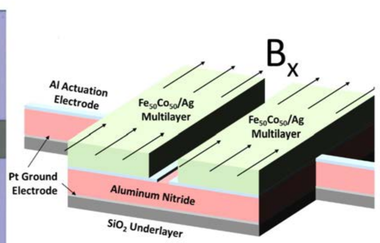

Figure 4: ME Device image (left) and layered schematic (right) [4].

ME Effect

- Mechanically coupled MS and PE material layers
- Convert external magnetic fields to current
- MS layer strains from magnetic field
- Strain transferred to PE layer, creating detectable voltage change

Resonance

- Sensitivity maximized when device is driven at one of two resonant frequency modes
  - High frequency (~6.5 MHz) extensional mode, high Q-factor allows biosensing capabilities
  - Low frequency (~70 kHz) bending mode, in range for safe higher power WPT

ME Optimization

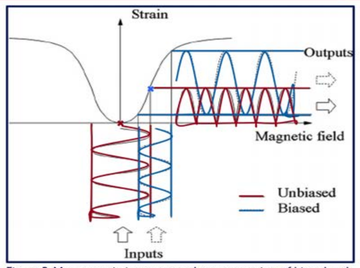

Figure 5: Magnetostriction curve and representation of biased and unbiased inputs with respective outputs [5]

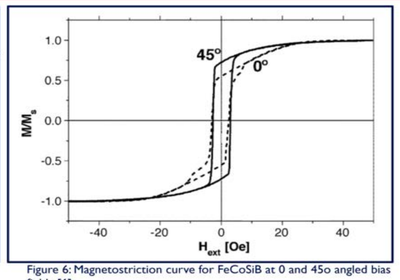

Figure 6: Magnetostriction curve for FeCoSiB at 0 and 45o angled bias fields [6].

Goal

- Create highest change in strain per change in magnetic field as shown in Figure 5
- Allowing high sensitivity to AC signals

Methods of Optimization

- Exploring different materials at different stresses
- DC Biasing
  - Orient MS dipoles so they rotate easily
  - **Magnitude**: Previously shown to improve MS performance
  - **Angle**: Some MS materials show best response at 45^o, shown in Figure 6 in FeCoSiB:

Device Testing Methods

Electrical Testing

- Vector network analyzer (VNA) was used to take S21 measurements
- Tests efficacy of PE layer
- Used to find:
  - Quality factor, $Q = \frac{Energy\ Stored}{Energy\ Lost} = \frac{f_0}{\Delta f}$
  - Resonant frequency for both modes

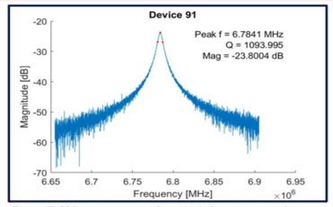

Figure 7: S21 measurement from high frequency mode

Magnetic Testing Redesign

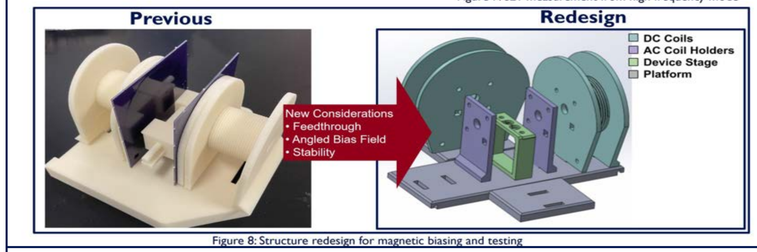

Figure 8: Structure redesign for magnetic biasing and testing

AC Signal Coils

- Generate signals to be sensed by device
  - Mimicking biomagnetic signals
  - WPT signals
- Range of operation is 1Hz -13MHz
  - Found using Smith Chart shown in Figure 9.
- 50% size, 200% power compared to previous coils

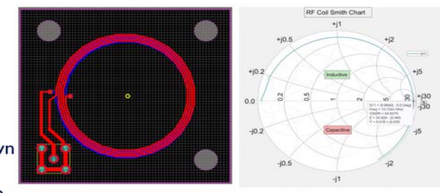

Figure 9: PCB coil design for AC signals (left) and Smith Chart coil characterization (right).

DC Bias Coils

- Designed to produce a varied angle and magnitude by changing current to each coil set.
- Perpendicular coil sets to allow for B_{eff} to occur at angle Θ_{eff}
- Each coil
  - 125 turns
  - ~0.36 Ω

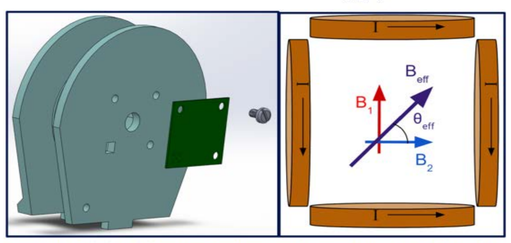

Figure 10: DC Coil (left) and coil configuration for generating angled DC bias field.

Results

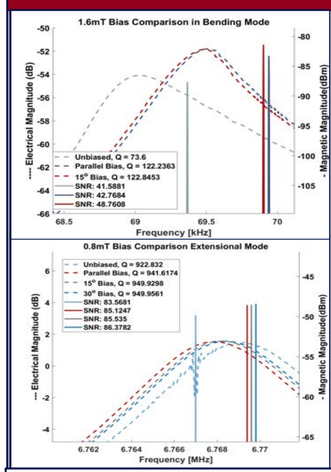

Bending Mode (~70kHz)

- At 1.6mT Bias Magnitude
  - Q-factor increases from unbiased to biased
  - SNR is 6 dBm (2x) greater in 15° DC bias than parallel
- Shown in Figure 12
  - Q-factor increases with DC Bias magnitude
  - Magnetic response increases slightly with angles of 15° and 30° from parallel

Extensional Mode (~6.76 MHz)

- At 0.8mT Bias Magnitude
  - Q-factor increases from unbiased to biased
  - SNR increases with bias magnitude rather than angle
- Shown in Figure 12
  - Q-factor increases with DC Bias magnitude
  - Magnetic response not significantly correlated to angle

Figure 11: Comparison of unbiased, parallel biased and angled bias in bending mode (top) and extensional mode (bottom).

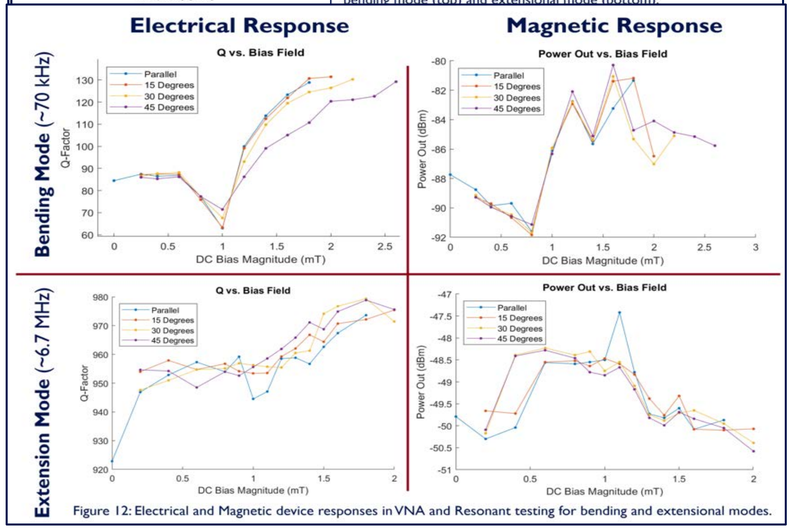

Figure 12: Electrical and Magnetic device responses in VNA and Resonant testing for bending and extensional modes.

Conclusion

Project Outcomes

- Ability to generate AC signals that mimic biomagnetic and WPT transmission signals
- Successful Testing structure for angled bias field
- Indication that parallel DC bias field is not always optimal for MS materials
- Insight into relationships between magnetic and electrical responses

Future Steps

- Different materials: Galfenol was the target MS material for angled testing, not Iron Cobalt
- Testing with other device types
- Addition of Hall Effect sensors into testing structure to continuously characterize the DC bias field

7) References

[1] Zuo, Siming, et al. "Modelling and Analysis of Magnetic Fields from Skeletal Muscle for Valuable Physiological Measurements." arXiv preprint arXiv:2104.02036 (2021).
[2] IEEE Standard for Safety Levels with Respect to Human Exposure to Radio Frequency Electromagnetic Fields, 3kHz to 300GHz", IEEE C95.1-1991
[3] "Piezoelectricity in Quartz." [Online]. Available: https://dev.nsta.org/evwebs/2014102/news/default.html. [Accessed: 29-Jul-2022].
[4] M. D'Agati, S. Sofronici, Yujia Huo, R. H. Olsson III, P. Finkel, K. Bussmann, T. Mion, M. Staruch, K. McLaughlin, B. Wheeler. "High-Q Factor, Multiferroic Resonant Magnetic Field Sensors and Limits on Strain Modulated Sensing Performance," to be published.
[5] Zhou, Nanjia & Blatchley, Charles & Ibeh, Christopher. (2009). Design and construction of a novel rotary magnetostrictive motor. Journal of Applied Physics. 105. 07F113 - 07F113. 10.1063/1.3076896.
[6] M. Frommberger, J. McCord and E. Quandt, "High-frequency properties of FeCoSiB thin films with crossed anisotropy," in IEEE Transactions on Magnetics, vol. 40, no. 4, pp. 2703-2705, July 2004, doi: 10.1109/TMAG.2004.832139.

8) Acknowledgements

I would like to thank Sydney Sofronici, Michael D'Agati, Dr. Troy Olsson, and the entire Olsson group at the University of Pennsylvania for the everything they taught me and helped me accomplish so far this summer. Additional thanks the National Science Foundation for funding the SUNFEST program with NSF REU grant no. 1950720, Dr. Sue-Ann Bidstrup Allen and Julia Falcon of the University of Pennsylvania for organizing the SUNFEST REU, and the Biomedical Library's Printing Center for 3D printed structures.